On the Passivity of Polynomial Chaos-Based Augmented Models for Stochastic Circuits

Paolo Manfredi, *Student Member, IEEE,* Dries Vande Ginste, *Senior Member, IEEE,*
Daniël De Zutter, *Fellow, IEEE,* Flavio G. Canavero, *Fellow, IEEE*

***Abstract*—This paper addresses for the first time the issue of passivity of the circuit models produced by means of the generalized polynomial chaos technique in combination with the stochastic Galerkin method. This approach has been used in literature to obtain statistical information through the simulation of an augmented but deterministic instance of a stochastic circuit, possibly including distributed transmission-line elements. However, transient simulations raise the critical question as to whether such an augmented network is passive or not. This paper discusses the general requirements for the augmented circuits to be passive and provides a sufficient condition for their passivity. Some numerical examples illustrate the theoretical results and conclude the paper.**

***Index Terms*—Lumped circuits, passivity, polynomial chaos, stochastic analysis, transmission lines, uncertainty.**

I. Introduction

The growing demand for large-scale integration and stringent design specifications of electronic systems are making the impact of variability of circuit parameters increasingly relevant and hard to control. Because of this, in recent years, the electrical engineering community has been calling for expedite and reliable stochastic modeling techniques to assess variability in the early design phase (e.g., [1]–[3]). The traditional, brute-force and blind Monte Carlo (MC) method is based on the repeated solution of a system for different values of the design parameters, sampled according to their distribution. The problem is not tractable whenever the computational cost of each simulation is high, as it is known to require a large number of samples to converge [4]. Improved techniques such as Latin hypercube sampling [5] and quasi Monte Carlo [6] have been proposed to accelerate the convergence, but their applicability is limited due to restrictions in the design of such methods.

On the other hand, there exist techniques which take advantage of a possible smoothness of the random parameters. In this framework, the generalized polynomial chaos (gPC) approach [7] turned out to be extremely appealing and has been used for the simulation of electronic circuits and their interconnections [8]–[14]. Briefly speaking, the gPC technique is based on the expansion of random system outputs in terms of suitable orthogonal polynomials. It can be split into two classes, based on the methodology for the computation of the coefficients of such expansions: the stochastic collocation methods (SCMs) interpolate a reduced set of system responses computed for properly-chosen samples of the random space, while the stochastic Galerkin method (SGM) amounts to modifying the governing equations in order to obtain a larger but deterministic system, whose solution provides the sought-for coefficients [15]. The latter requires just one single system simulation and turns out to be particularly suitable whenever the governing equations are reasonably simple to manipulate. The result is a deterministic, stand-alone model inherently including the effects of parameter variations.

P. Manfredi and F. Canavero are with the Dipartimento di Elettronica e Telecomunicazioni, EMC Group, Politecnico di Torino, Torino 10129, Italy (e-mail: paolo.manfredi@polito.it; flavio.canavero@polito.it).

D. Vande Ginste and D. De Zutter are with the Department of Information Technology, Electromagnetics Group, Ghent University, Ghent 9000, Belgium (e-mail: dries.vandeginste@ugent.be; daniel.dezutter@ugent.be).

The authors of this paper presented an application of the gPC approach, in conjunction with the SGM, to the analysis of distributed interconnects described by transmission-line equations and affected by uncertainties in their geometric and material properties [16]–[18]. The result is an augmented, deterministic set of transmission-line equations, whose solution can capture the effects of parameter variations much faster than running a large number of MC simulations. In [19]–[21], the methodology has been extended to the time-domain analysis in a SPICE-like environment, where a circuit interpretation was given to the new equations and the inclusion of stochastic lumped elements was addressed as well. A deterministic, though augmented, instance of the original circuit is created, where stochastic elements are replaced by deterministic larger multi-terminal elements or subcircuits. However, especially when performing transient simulations, the creation of circuit models from passive systems raises the fundamental question as to whether the passivity is preserved or not [22]. The present paper addresses this issue for the gPC-based circuit models generated from linear electrical networks consisting of stochastic lumped and distributed elements. Nonetheless, as the discussion is based on energy considerations, it may in the future be generalized to other classes of equations in different domains.

This paper is organized as follows. Section II provides an overview of the application of the gPC to linear circuits consisting of both distributed and lumped elements. In Section III, the necessary conditions for the resulting augmented models to be passive are enumerated. In Section IV, these general criteria are linked to the properties of the gPC expansions and a sufficient condition for passivity is outlined. The theory is illustrated by meaningful, numerical examples in Section V. Finally, conclusions are drawn in Section VI.

II. Polynomial Chaos and Linear Circuits

This section summarizes the key steps in the application of the gPC and SGM to the stochastic analysis of linear electrical networks. A thorough analysis of the gPC-based approach in terms of accuracy and computational time is out of the scope of this paper. For an exhaustive discussion in this regard, readers are referred to [16]–[21] and references therein. For the sake of consistency with the references, in the present paper the discussion is also presented in the Laplace domain.

A. Inclusion of Distributed Transmission-Line Elements

When the geometrical and/or material properties of multiconductor transmission lines are affected by random uncertainties, their per-unit-length (p.u.l.) matrices become stochastic. By collecting the random variables responsible for variability into a multivariate vector $\boldsymbol{\xi} = [\xi_1, \ldots, \xi_n]$, where n is the number of independent uncertain parameters, the pertinent stochastic telegrapher's equations for a multiconductor transmission line consisting of N signal conductors and a reference conductor can be expressed as

$$\frac{d}{dz}\mathbf{V}(z,s,\boldsymbol{\xi}) = -\mathbf{Z}_{\mathrm{pul}}(s,\boldsymbol{\xi})\mathbf{I}(z,s,\boldsymbol{\xi}), \tag{1a}$$

$$\frac{d}{dz}\mathbf{I}(z,s,\boldsymbol{\xi}) = -\mathbf{Y}_{\mathrm{pul}}(s,\boldsymbol{\xi})\mathbf{V}(z,s,\boldsymbol{\xi}), \tag{1b}$$

where s is the Laplace variable, z is the direction of propagation, $\mathbf{Z}_{\mathrm{pul}}(s,\boldsymbol{\xi}) = \mathbf{R}_{\mathrm{pul}}(\boldsymbol{\xi}) + s\mathbf{L}_{\mathrm{pul}}(\boldsymbol{\xi})$ and $\mathbf{Y}_{\mathrm{pul}}(s,\boldsymbol{\xi}) = \mathbf{G}_{\mathrm{pul}}(\boldsymbol{\xi}) + s\mathbf{C}_{\mathrm{pul}}(\boldsymbol{\xi})$ are the p.u.l. impedance and admittance $(N \times N)$-matrices, respectively. These latter are sometimes split in their p.u.l. resistance ($\mathbf{R}_{\mathrm{pul}}$), inductance ($\mathbf{L}_{\mathrm{pul}}$), conductance ($\mathbf{G}_{\mathrm{pul}}$) and capacitance ($\mathbf{C}_{\mathrm{pul}}$). Note that in the sequel, the subscript "pul" is omitted for brevity of notation. It will always be clear from the context whether distributed or lumped elements are discussed.

In the above equation, the randomness of the p.u.l. matrices is emphasized by their dependence on the random vector $\boldsymbol{\xi}$. Furthermore, it is worth noting that the variability in turn also affects the voltages and currents along the line, collected into the N-vectors $\mathbf{V}$ and $\mathbf{I}$, which therefore depend on $\boldsymbol{\xi}$ as well.

The gPC approach consists of two main steps: first, the stochastic p.u.l. matrices in (1) are expressed in terms of a truncated series of $P+1$ multivariate orthogonal polynomials $\{\phi_k\}$:

$$\mathbf{Z}(s,\boldsymbol{\xi}) \approx \hat{\mathbf{Z}}(s,\boldsymbol{\xi}) = \sum_{k=0}^{P} \mathbf{Z}_k(s)\phi_k(\boldsymbol{\xi}), \tag{2a}$$

$$\mathbf{Y}(s,\boldsymbol{\xi}) \approx \hat{\mathbf{Y}}(s,\boldsymbol{\xi}) = \sum_{k=0}^{P} \mathbf{Y}_k(s)\phi_k(\boldsymbol{\xi}), \tag{2b}$$

where $\mathbf{Z}_k(s) = \mathbf{R}_k + s\mathbf{L}_k$ and $\mathbf{Y}_k(s) = \mathbf{G}_k + s\mathbf{C}_k$ are deterministic matrix coefficients. The total number of expansion terms is given by $P+1 = (p+n)!/p!n!$, where p is the selected order of the approximation. Although an a-priori criterion for the order selection does not exist, we proved in [19]–[21] that choosing $p = 2$ generally provides satisfactory simulation accuracy.

As the polynomials $\{\phi_k\}$ are chosen to be orthogonal with respect to the following inner product

$$\langle f(\boldsymbol{\xi}), g(\boldsymbol{\xi})\rangle = \int_{\mathbb{R}^n} f(\boldsymbol{\xi})g(\boldsymbol{\xi})w(\boldsymbol{\xi})d\boldsymbol{\xi}, \tag{3}$$

where $w(\boldsymbol{\xi})$ is a weighting function coinciding with the joint probability density function of $\boldsymbol{\xi}$, the above coefficients can be readily computed as

$$\mathbf{Z}_k(s) = \frac{\langle \mathbf{Z}(s,\boldsymbol{\xi}), \phi_k(\boldsymbol{\xi})\rangle}{\langle \phi_k(\boldsymbol{\xi}), \phi_k(\boldsymbol{\xi})\rangle}, \tag{4a}$$

$$\mathbf{Y}_k(s) = \frac{\langle \mathbf{Y}(s,\boldsymbol{\xi}), \phi_k(\boldsymbol{\xi})\rangle}{\langle \phi_k(\boldsymbol{\xi}), \phi_k(\boldsymbol{\xi})\rangle}. \tag{4b}$$

The unknown voltages and currents are expanded in a similar fashion:

$$\mathbf{V}(z,s,\boldsymbol{\xi}) \approx \hat{\mathbf{V}}(z,s,\boldsymbol{\xi}) = \sum_{k=0}^{P} \mathbf{V}_k(z,s)\phi_k(\boldsymbol{\xi}), \tag{5a}$$

$$\mathbf{I}(z,s,\boldsymbol{\xi}) \approx \hat{\mathbf{I}}(z,s,\boldsymbol{\xi}) = \sum_{k=0}^{P} \mathbf{I}_k(z,s)\phi_k(\boldsymbol{\xi}), \tag{5b}$$

where the coefficients $\mathbf{V}_k$ and $\mathbf{I}_k$ become the new unknowns of the problem. Substitution of (2) and (5) into (1) yields

$$\begin{aligned}\frac{d}{dz}\sum_{k=0}^{P} \mathbf{V}_k(z,s)\phi_k(\boldsymbol{\xi}) \\ = -\sum_{k=0}^{P}\sum_{j=0}^{P} \mathbf{Z}_k(s)\mathbf{I}_j(z,s)\phi_k(\boldsymbol{\xi})\phi_j(\boldsymbol{\xi}),\end{aligned} \tag{6a}$$

$$\begin{aligned}\frac{d}{dz}\sum_{k=0}^{P} \mathbf{I}_k(z,s)\phi_k(\boldsymbol{\xi}) \\ = -\sum_{k=0}^{P}\sum_{j=0}^{P} \mathbf{Y}_k(s)\mathbf{V}_j(z,s)\phi_k(\boldsymbol{\xi})\phi_j(\boldsymbol{\xi}).\end{aligned} \tag{6b}$$

It should be observed that (6), like (1), is still a stochastic problem, albeit approximated in terms of (2) and (5). Therefore, the second step involves the application of Galerkin projection, i.e. (6) is weighed with the same set of polynomials $\{\phi_k\}$, $k = 0, \ldots, P$, using the inner product (3). This leads to a set of $P+1$ transmission-line-like equations, which can be cast in matrix form, as follows:

$$\frac{d}{dz}\tilde{\mathbf{V}}(z,s) = -\tilde{\mathbf{Z}}(s)\tilde{\mathbf{I}}(z,s), \tag{7a}$$

$$\frac{d}{dz}\tilde{\mathbf{I}}(z,s) = -\tilde{\mathbf{Y}}(s)\tilde{\mathbf{V}}(z,s), \tag{7b}$$

where $\tilde{\mathbf{Z}}(s) = \tilde{\mathbf{R}} + s\tilde{\mathbf{L}}$ and $\tilde{\mathbf{Y}}(s) = \tilde{\mathbf{G}} + s\tilde{\mathbf{C}}$ are $N(P+1) \times N(P+1)$ p.u.l. matrices, organized into $(P+1) \times (P+1)$ blocks, each block given by

$$\tilde{\mathbf{Z}}_{ij}(s) = \sum_{k=0}^{P} \mathbf{Z}_k(s)\alpha_{kji}, \tag{8a}$$

$$\tilde{\mathbf{Y}}_{ij}(s) = \sum_{k=0}^{P} \mathbf{Y}_k(s)\alpha_{kji}, \tag{8b}$$

$(i, j = 0, \ldots, P)$, with

$$\alpha_{kji} = \frac{\langle \phi_k(\boldsymbol{\xi})\phi_j(\boldsymbol{\xi}), \phi_i(\boldsymbol{\xi})\rangle}{\langle \phi_i(\boldsymbol{\xi}), \phi_i(\boldsymbol{\xi})\rangle}. \tag{9}$$

It is important noting that (7) amounts to a *deterministic* system of differential equations, thanks to the Galerkin projection which eliminates the random variable $\boldsymbol{\xi}$ from (6). Thus, (7) requires a single solution of an augmented system, which is generally much faster than running a large number of MC simulations. The unique solution of (7) provides the sought-for coefficients for the voltages and currents, which are collected into the new unknowns $\tilde{\mathbf{V}} = [\mathbf{V}_0, \ldots, \mathbf{V}_P]^T$ and $\tilde{\mathbf{I}} = [\mathbf{I}_0, \ldots, \mathbf{I}_P]^T$, respectively. Moreover, the knowledge of the coefficients for the voltage and current variables allows to quickly extract their statistical information from (5).

Numerically solving (7) can be easily carried out in, e.g., Matlab [16]–[18]. However, a SPICE-type circuit implementation allows to deal with more complex networks consisting of many, possibly stochastic, elements. The augmented transmission lines can be simulated by means of existing models for multiconductor lines, such as the W-element available in HSPICE or Agilent's ADS [21]. Fig. 1 visualizes the procedure for the application of the gPC to transmission-line elements in the case $N = 2$ and $P = 2$: every stochastic line, described by the pertinent p.u.l. parameters $\mathbf{Z}$ and $\mathbf{Y}$, is "expanded" into a deterministic one, having a larger number of terminals, and described by $\tilde{\mathbf{Z}}$ and $\tilde{\mathbf{Y}}$. Of course, the augmented lines have no real physical counterpart.

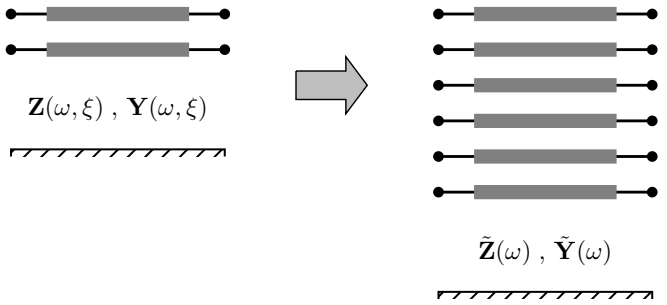

Fig. 1. Pictorial illustration of the procedure for the construction of the augmented transmission-line elements, for the case $N = 2$ and $P = 2$.

B. Inclusion of Lumped Elements

As to classical lumped circuit elements, i.e., resistors, capacitors and inductors, that exhibit random variations, new deterministic equations are obtained by means of a procedure similar to the one outlined in the previous section for distributed elements [19]. For the sake of brevity, we limit ourselves here to summarizing the results. The stochastic constitutive equations for resistances, conductances, inductances and capacitances, i.e.

$$V(s, \boldsymbol{\xi}) = R(\boldsymbol{\xi})I(s, \boldsymbol{\xi}), \tag{10}$$

$$V(s, \boldsymbol{\xi}) = sL(\boldsymbol{\xi})I(s, \boldsymbol{\xi}), \tag{11}$$

$$I(s, \boldsymbol{\xi}) = G(\boldsymbol{\xi})V(s, \boldsymbol{\xi}), \tag{12}$$

$$I(s, \boldsymbol{\xi}) = sC(\boldsymbol{\xi})V(s, \boldsymbol{\xi}), \tag{13}$$

respectively, are expanded into corresponding deterministic matrix equations, as follows

$$\tilde{\mathbf{V}}(s) = \tilde{\mathbf{R}}\tilde{\mathbf{I}}(s), \tag{14}$$

$$\tilde{\mathbf{V}}(s) = s\tilde{\mathbf{L}}\tilde{\mathbf{I}}(s), \tag{15}$$

$$\tilde{\mathbf{I}}(s) = \tilde{\mathbf{G}}\tilde{\mathbf{V}}(s), \tag{16}$$

$$\tilde{\mathbf{I}}(s) = s\tilde{\mathbf{C}}\tilde{\mathbf{V}}(s), \tag{17}$$

where the entries of the augmented $(P+1)\times(P+1)$ matrices $\tilde{\mathbf{R}}$, $\tilde{\mathbf{L}}$, $\tilde{\mathbf{G}}$, $\tilde{\mathbf{C}}$ are analogous to (8).

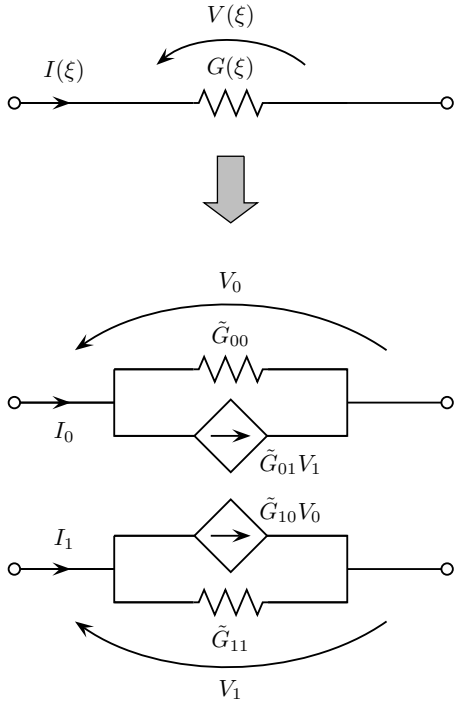

Fig. 2. Practical implementation of the multi-terminal circuit described by (16) for the case $P = 1$.

It should be noted that (14)–(17) define the behavior of $P + 1$ branches, relating the currents flowing into them to the voltages across them. As an illustrative example, Fig. 2 shows a possible circuit implementation of (16) in the case $P = 1$, where dependent sources are introduced to model the off-diagonal matrix elements (a similar approach can be used also for the other element types). Again, there is here no physical meaning attached to the electrical parameters appearing in the circuit interpretation of the gPC-augmented equations. Also, the symmetry of the matrices in (7) and (14)–(17) is guaranteed only by the adoption of an *orthonormal*, rather than simply orthogonal, set of basis functions. This choice is a fundamental step for the gPC-based circuit simulation inside standard design environments [23], and introduces symmetry in the augmented transmission-line models as well as in the structure of the subcircuits implementing the new constitutive equations for lumped elements (cfr. for instance Fig. 2, with $G_{01} = G_{10}$). This in turn preserves the symmetry of the pertinent impedance, admittance or state-space representations, and therefore reciprocity. In this regard, we remark that the

possible presence of dependent sources does not necessarily imply the loss of reciprocity [24].

Once the new augmented matrices are known, the overall gPC system can be topologically considered as a larger, deterministic electrical network, where each node in the original circuit is expanded into $P+1$ nodes and each stochastic element is replaced, as illustrated in Figs. 1 and 2, by a deterministic multi-terminal element, which implements the corresponding augmented constitutive equations. The new circuit variables are the gPC coefficients for the original, stochastic voltages and currents. Despite the increased network size, the pertinent statistical information is readily extracted from the gPC expansions after a single circuit simulation, thus making this approach far more efficient than performing a large number of MC runs.

The solution of the resulting augmented circuit can be computed by means of any SPICE-like software. This choice also provides a convenient way to compute time-domain results, but definitely gives rise to the question as to whether the new network is passive or not. It is relevant to remark that the circuit implementation of (7) and (14)–(17), which is achieved by means of standard components, implies that a classical interpretation in terms of voltage and current variables is given to the unknown gPC coefficients. As such, classical energy considerations for passive circuits apply to the augmented models as well.

III. Passivity of the Augmented Circuit Models

A circuit is denoted as passive when it is unable to generate energy [22]. In this section, the conditions for the equivalent circuit models for (7) and (14)–(17) to be passive are enumerated, based on energy considerations. The passivity of larger netlists, comprising many of these building blocks, is guaranteed by the fact that the concatenation of passive circuits yields a passive network.

Before continuing, we first introduce the time-domain counterparts of (7) and (14)–(17), which are obtained via inverse Laplace transform, i.e.

$$\frac{\partial}{\partial z}\tilde{\mathbf{v}}(z,t) = -\tilde{\mathbf{R}}\tilde{\mathbf{i}}(z,t) - \tilde{\mathbf{L}}\frac{\partial}{\partial t}\tilde{\mathbf{i}}(z,t), \tag{18a}$$

$$\frac{\partial}{\partial z}\tilde{\mathbf{i}}(z,t) = -\tilde{\mathbf{G}}\tilde{\mathbf{v}}(z,t) - \tilde{\mathbf{C}}\frac{\partial}{\partial t}\tilde{\mathbf{v}}(z,t), \tag{18b}$$

and

$$\tilde{\mathbf{v}}(t) = \tilde{\mathbf{R}}\tilde{\mathbf{i}}(t), \tag{19}$$

$$\tilde{\mathbf{v}}(t) = \tilde{\mathbf{L}}\frac{d}{dt}\tilde{\mathbf{i}}(t), \tag{20}$$

$$\tilde{\mathbf{i}}(t) = \tilde{\mathbf{G}}\tilde{\mathbf{v}}(t), \tag{21}$$

$$\tilde{\mathbf{i}}(t) = \tilde{\mathbf{C}}\frac{d}{dt}\tilde{\mathbf{v}}(t), \tag{22}$$

respectively, where $\tilde{\mathbf{v}} = \mathcal{L}^{-1}\{\tilde{\mathbf{V}}\}$ and $\tilde{\mathbf{i}} = \mathcal{L}^{-1}\{\tilde{\mathbf{I}}\}$, operator $\mathcal{L}$ denoting the Laplace transform.

A. Augmented Transmission-Line Equations

The circuit interpretation of (18) as a classical transmission-line system implies that it is possible to define the spatial variation of the total propagating power as

$$\begin{aligned}\frac{\partial}{\partial z}p(z,t) &= \frac{\partial}{\partial z}[\tilde{\mathbf{v}}^T(z,t)\tilde{\mathbf{i}}(z,t)] \\ &= -\tilde{\mathbf{i}}^T(z,t)\tilde{\mathbf{R}}\tilde{\mathbf{i}}(z,t) - \frac{\partial}{\partial t}\tilde{\mathbf{i}}^T(z,t)\tilde{\mathbf{L}}\tilde{\mathbf{i}}(z,t) \\ &\quad -\tilde{\mathbf{v}}^T(z,t)\tilde{\mathbf{G}}\tilde{\mathbf{v}}(z,t) - \frac{\partial}{\partial t}\tilde{\mathbf{v}}^T(z,t)\tilde{\mathbf{C}}\tilde{\mathbf{v}}(z,t),\end{aligned} \tag{23}$$

where we have made use of the symmetry of $\tilde{\mathbf{R}}$, $\tilde{\mathbf{L}}$, $\tilde{\mathbf{G}}$ and $\tilde{\mathbf{C}}$. The total absorbed p.u.l. energy is the integral over time of the opposite of the above quantity, i.e. $-\frac{\partial}{\partial z}p(z,t)$, and can be split into two components:

$$w_{\mathrm{diss}} = \int_{-\infty}^{t}[\tilde{\mathbf{i}}^T(z,\tau)\tilde{\mathbf{R}}\tilde{\mathbf{i}}(z,\tau) + \tilde{\mathbf{v}}^T(z,\tau)\tilde{\mathbf{G}}\tilde{\mathbf{v}}(z,\tau)]d\tau \tag{24}$$

and

$$\begin{aligned}w_{\mathrm{em}} &= \int_{-\infty}^{t}[\frac{d}{d\tau}\tilde{\mathbf{i}}^T(z,\tau)\tilde{\mathbf{L}}\tilde{\mathbf{i}}(z,\tau) + \frac{d}{d\tau}\tilde{\mathbf{v}}^T(z,\tau)\tilde{\mathbf{C}}\tilde{\mathbf{v}}(z,\tau)]d\tau \\ &= \frac{1}{2}\tilde{\mathbf{i}}^T(z,t)\tilde{\mathbf{L}}\tilde{\mathbf{i}}(z,t) + \frac{1}{2}\tilde{\mathbf{v}}^T(z,t)\tilde{\mathbf{C}}\tilde{\mathbf{v}}(z,t),\end{aligned} \tag{25}$$

where we used the property

$$\frac{d}{d\tau}\tilde{\mathbf{i}}^T(z,\tau)\tilde{\mathbf{L}}\tilde{\mathbf{i}}(z,\tau) = \frac{1}{2}\frac{d}{d\tau}[\tilde{\mathbf{i}}^T(z,\tau)\tilde{\mathbf{L}}\tilde{\mathbf{i}}(z,\tau)], \tag{26}$$

valid when $\tilde{\mathbf{L}}$ is symmetric and assuming that $\tilde{\mathbf{v}}(t = -\infty), \tilde{\mathbf{i}}(t = -\infty) = \mathbf{0}$. A similar relation holds for $\tilde{\mathbf{v}}$ and $\tilde{\mathbf{C}}$. For physical transmission lines, (24) represents the p.u.l. energy dissipated into the conductors and embedding material, whereas (25) is the p.u.l. energy stored in the electromagnetic field [25], [26].

In order for the system (18) not to generate energy, both (24) and (25) must be positive for every voltage and current configuration, at any location z along the line and at any time t. In fact, this is guaranteed only if $\tilde{\mathbf{R}}$, $\tilde{\mathbf{L}}$, $\tilde{\mathbf{G}}$ and $\tilde{\mathbf{C}}$ are all positive-definite (PD) matrices. We recall that a real and symmetric $m \times m$ matrix $\mathbf{M}$ is said to be PD if the following inequality

$$\mathbf{x}^T\mathbf{M}\mathbf{x} > 0 \tag{27}$$

holds for any arbitrary, non-null choice of the vector $\mathbf{x} \in \mathbb{R}^m$. In our case, i.e. (24) and (25), we have $m = N(P+1)$.

However, whereas the above condition is always satisfied for physical lines, this is not readily the case for their gPC-augmented counterparts. So far, a proof of passivity for augmented lines has not been presented.

B. Augmented Equations for Lumped Elements

Let us start from the time-domain augmented conductance equation (21). The total power dissipated by the corresponding multi-terminal circuit element (see Fig. 2) is the sum of the powers dissipated in each branch, i.e.

$$p(t) = \sum_{i=0}^{P} v_i(t)i_i(t) = \tilde{\mathbf{v}}^T(t)\tilde{\mathbf{i}}(t) = \tilde{\mathbf{v}}^T(t)\tilde{\mathbf{G}}\tilde{\mathbf{v}}(t). \tag{28}$$

Once again, the passivity condition requires such power to be positive regardless of the voltage values, i.e. $\tilde{\mathbf{G}}$ has to be PD. A similar condition can be derived for the resistance equation (19), for which the dissipated power is given by

$$p(t) = \tilde{\mathbf{i}}^T(t)\tilde{\mathbf{R}}\tilde{\mathbf{i}}(t). \tag{29}$$

As to the circuit models for (20) and (22), analogous steps allow to obtain the following expressions for the energy:

$$w_C(t) = \frac{1}{2}\tilde{\mathbf{v}}^T(t)\tilde{\mathbf{C}}\tilde{\mathbf{v}}(t), \tag{30}$$

$$w_L(t) = \frac{1}{2}\tilde{\mathbf{i}}^T(t)\tilde{\mathbf{L}}\tilde{\mathbf{i}}(t). \tag{31}$$

The latter expression is analogous to the energy stored in a set of mutually coupled inductors. In summary, the passivity conditions for the gPC models for lumped elements are similar to those for the augmented transmission lines, i.e., the corresponding augmented matrices must be PD. It is very important to remark at this point that the fact that the augmented matrices have to be PD, is completely independent from possible alternative ways in which equivalent circuit representations could be given for (7) or (14)–(17). E.g., in Fig. 2, the circuit representation of (16) used dependent current sources, but an alternative representation using dependent voltage sources is easily derived. Nonetheless, the only thing that remains mandatory is that $\tilde{\mathbf{G}}$ is PD.

IV. Positive-Definiteness of the Augmented Matrices

In the previous section, we showed that the new deterministic equations describe passive circuit models if the corresponding augmented matrices are PD. In this section, we provide a sufficient condition for such matrices to be PD, which stems from the properties of the original, stochastic parameters, and of the gPC representation. First, we present the proof for equations that are originally scalar, like those for lumped circuit elements (10)–(13) or single transmission lines, i.e. (1) with $N = 1$. Next, the result is extended to matrix equations like multiconductor telegrapher's equations ($N > 1$).

A. Proof for Lumped Equations and Single Lines

Suppose we have a scalar random parameter $A(\boldsymbol{\xi})$, which is expanded like in (2):

$$A(\boldsymbol{\xi}) \approx \hat{A}(\boldsymbol{\xi}) = \sum_{k=0}^{P} A_k \phi_k(\boldsymbol{\xi}). \tag{32}$$

Clearly, A can be a lumped random element in (10)–(13), or any of the four random p.u.l. parameters of a single transmission line. By combining (8) with (9), the entries of the corresponding augmented matrix $\tilde{\mathbf{A}}$ can be expressed as

$$\tilde{A}_{ij} = \sum_{k=0}^{P} A_k \langle \phi_k(\boldsymbol{\xi})\phi_j(\boldsymbol{\xi}), \phi_i(\boldsymbol{\xi})\rangle, \tag{33}$$

where the denominator of (9) is now made unitary thanks to the choice of normalized polynomials (rendering $\tilde{A}_{ij} = \tilde{A}_{ji}$). Using the linearity of inner products, (33) can be rewritten as

$$\tilde{A}_{ij} = \langle \sum_{k=0}^{P} A_k \phi_k(\boldsymbol{\xi})\phi_j(\boldsymbol{\xi}), \phi_i(\boldsymbol{\xi})\rangle = \langle \hat{A}(\boldsymbol{\xi})\phi_j(\boldsymbol{\xi}), \phi_i(\boldsymbol{\xi})\rangle. \tag{34}$$

In order to be PD, $\tilde{\mathbf{A}}$ has to satisfy (27). We have

$$\begin{aligned}
\mathbf{x}^T\tilde{\mathbf{A}}\mathbf{x} &= \sum_{i=0}^{P}\sum_{j=0}^{P} x_i \tilde{A}_{ij} x_j \\
&= \sum_{i=0}^{P}\sum_{j=0}^{P} x_i x_j \langle \hat{A}(\boldsymbol{\xi})\phi_j(\boldsymbol{\xi}), \phi_i(\boldsymbol{\xi})\rangle \\
&= \sum_{i=0}^{P} x_i \langle \hat{A}(\boldsymbol{\xi}) \sum_{j=0}^{P} x_j \phi_j(\boldsymbol{\xi}), \phi_i(\boldsymbol{\xi})\rangle \\
&= \langle \sum_{i=0}^{P} x_i \phi_i(\boldsymbol{\xi}), \hat{A}(\boldsymbol{\xi}) \sum_{j=0}^{P} x_j \phi_j(\boldsymbol{\xi})\rangle,
\end{aligned} \tag{35}$$

where we used the properties of linearity and symmetry of the inner product (3). We denote:

$$\sum_{i=0}^{P} x_i \phi_i(\boldsymbol{\xi}) = \sum_{j=0}^{P} x_j \phi_j(\boldsymbol{\xi}) = y(\boldsymbol{\xi}), \tag{36}$$

where $y(\boldsymbol{\xi})$ is merely a function given by a linear combination of the functions $\{\phi_i(\boldsymbol{\xi})\}$. It is worthwhile noting that, since the basis functions are linearly independent (they are orthogonal), $y(\boldsymbol{\xi})$ cannot be null if $\mathbf{x}$ is non-null. We now have

$$\mathbf{x}^T\tilde{\mathbf{A}}\mathbf{x} = \langle y(\boldsymbol{\xi}), \hat{A}(\boldsymbol{\xi})y(\boldsymbol{\xi})\rangle. \tag{37}$$

Recalling the definition (3) of the inner product in the gPC framework, it is possible to write

$$\mathbf{x}^T\tilde{\mathbf{A}}\mathbf{x} = \int_{\mathbb{R}^n} y^2(\boldsymbol{\xi})\hat{A}(\boldsymbol{\xi})w(\boldsymbol{\xi})d\boldsymbol{\xi}, \tag{38}$$

which is always positive if $\hat{A}(\boldsymbol{\xi}) > 0$, $\forall \boldsymbol{\xi}$. Note that $w(\boldsymbol{\xi})$ is always positive too, being a probability density function. Some considerations follow:

1) For the augmented matrix $\tilde{\mathbf{A}}$ to be PD, it is required that the approximated parameter $\hat{A}(\boldsymbol{\xi})$ is always positive in the considered domain of $\boldsymbol{\xi}$, i.e., that the approximation (32) retains the physical property of the original parameter $A(\boldsymbol{\xi})$ (for physical passive elements or single lines, resistances, inductances, conductances and capacitances are always positive). In other words, $\hat{A}(\boldsymbol{\xi})$ must still describe a passive element, which is — at least in hindsight — an understandable requirement.
2) The above condition is *sufficient*, but not *necessary*. In other words, even if it is not fulfilled, (38) can still be positive, although this is not guaranteed.
3) By taking an infinite series (i.e., $P \to \infty$), the approximation (32) becomes exact (the basis functions form a complete basis). Therefore, $\hat{A}$ is guaranteed to be positive and $\tilde{\mathbf{A}}$ is PD.
4) Denote

$$(f(\boldsymbol{\xi}), g(\boldsymbol{\xi})) = \int_{\mathbb{R}^n} f(\boldsymbol{\xi})g(\boldsymbol{\xi})\hat{A}(\boldsymbol{\xi})w(\boldsymbol{\xi})d\boldsymbol{\xi}. \tag{39}$$

If and only if $\hat{A}(\boldsymbol{\xi}) > 0$, $\forall \boldsymbol{\xi}$, the above equation defines another inner product in $\mathbb{R}^n$. The augmented matrix $\tilde{\mathbf{A}}$ is then a Gramian matrix, constructed using the linearly independent functions $\{\phi_k(\boldsymbol{\xi})\}$ and the inner product (39). This reasoning can be used as an alternative proof, since any Gramian matrix is PD.

B. Proof for Multiconductor Lines

In the case of multiconductor transmission lines ($N > 1$), the original stochastic system is described by matrix equations (1), with p.u.l. matrices that are PD. Each of these four matrices is expanded as (2):

$$\mathbf{A}(\boldsymbol{\xi}) \approx \hat{\mathbf{A}}(\boldsymbol{\xi}) = \sum_{k=0}^{P} \mathbf{A}_k \phi_k(\boldsymbol{\xi}). \tag{40}$$

We now exploit the fact that the corresponding augmented matrix $\tilde{\mathbf{A}}$ is a block matrix consisting of $(P+1) \times (P+1)$ blocks of size $N \times N$, with each block $\tilde{\mathbf{A}}_{ij}$ given by

$$\tilde{\mathbf{A}}_{ij} = \sum_{k=0}^{P} \mathbf{A}_k \langle \phi_k(\boldsymbol{\xi})\phi_j(\boldsymbol{\xi}), \phi_i(\boldsymbol{\xi})\rangle = \langle \hat{\mathbf{A}}(\boldsymbol{\xi})\phi_j(\boldsymbol{\xi}), \phi_i(\boldsymbol{\xi})\rangle. \tag{41}$$

So, (27) can be written as

$$\begin{aligned} \mathbf{x}^T \tilde{\mathbf{A}} \mathbf{x} &= \sum_{i=0}^{P}\sum_{j=0}^{P} \mathbf{x}_i^T \langle \hat{\mathbf{A}}(\boldsymbol{\xi})\phi_j(\boldsymbol{\xi}), \phi_i(\boldsymbol{\xi})\rangle \mathbf{x}_j \\ &= \sum_{i=0}^{P} \mathbf{x}_i^T \langle \hat{\mathbf{A}}(\boldsymbol{\xi}) \sum_{j=0}^{P} \mathbf{x}_j \phi_j(\boldsymbol{\xi}), \phi_i(\boldsymbol{\xi})\rangle \\ &= \langle \sum_{i=0}^{P} \mathbf{x}_i^T \phi_i(\boldsymbol{\xi}), \hat{\mathbf{A}}(\boldsymbol{\xi}) \sum_{j=0}^{P} \mathbf{x}_j \phi_j(\boldsymbol{\xi})\rangle, \end{aligned} \tag{42}$$

where $\mathbf{x}_i$ denotes the pertinent ith block of vector $\mathbf{x}$. Let us define

$$\sum_{i=0}^{P} \mathbf{x}_i \phi_i(\boldsymbol{\xi}) = \sum_{j=0}^{P} \mathbf{x}_j \phi_j(\boldsymbol{\xi}) = \mathbf{y}(\boldsymbol{\xi}), \tag{43}$$

which is merely a (non-null) N-vector whose entries are a linear combination of the functions $\{\phi_i(\boldsymbol{\xi})\}$. Therefore

$$\mathbf{x}^T \tilde{\mathbf{A}} \mathbf{x} = \langle \mathbf{y}^T(\boldsymbol{\xi}), \hat{\mathbf{A}}(\boldsymbol{\xi})\mathbf{y}(\boldsymbol{\xi})\rangle. \tag{44}$$

Again, recalling (3), we have

$$\langle \mathbf{y}^T(\boldsymbol{\xi}), \hat{\mathbf{A}}(\boldsymbol{\xi})\mathbf{y}(\boldsymbol{\xi})\rangle = \int_{\mathbb{R}^n} \mathbf{y}^T(\boldsymbol{\xi})\hat{\mathbf{A}}(\boldsymbol{\xi})\mathbf{y}(\boldsymbol{\xi}) w(\boldsymbol{\xi}) d\boldsymbol{\xi}, \tag{45}$$

which is always positive if and only if $\hat{\mathbf{A}}(\boldsymbol{\xi})$ is PD, $\forall \boldsymbol{\xi}$. Again, this means asking that the expansion (40) retains the property of positive definiteness which belongs to the original matrix $\mathbf{A}(\boldsymbol{\xi})$.

In conclusion, this section proves that the augmented matrix $\tilde{\mathbf{A}}$, whose entries are a combination of the smaller matrix $\hat{\mathbf{A}}$, inherits the positive definiteness property from this latter. Therefore, thanks to above result, the designer can assess the passivity upfront, before the augmented matrices and the corresponding circuit models are created. Although it is not possible to a-priori determine a specific expansion order which always guarantees $\tilde{\mathbf{A}}$ to be PD, in practical situations this condition can usually be met with a limited number of expansion terms, thanks to the optimal convergence of the gPC series. So, a straightforward procedure to produce passive circuit models is to increase the number of PC-expansion terms until $\hat{\mathbf{A}}$ is PD.

V. Numerical Examples

We now propose some illustrative examples of the theoretical results outlined in the previous sections. For illustration purposes, the proposed examples are deliberately simple. Nonetheless, as already discussed, the passivity of larger networks, consisting of many elements, originates directly from the passivity of their single circuit components. In the following, HSPICE will be used as a solution engine to perform transient simulations.

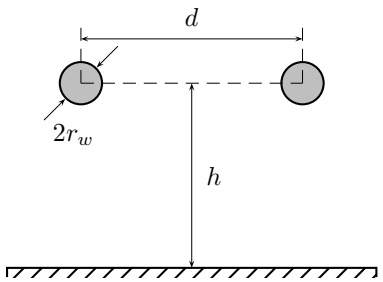

Fig. 3. Cross-section of a pair of coupled wires above a ground plane.

A. Pair of Coupled Transmission Lines

Consider a pair of coupled transmission lines ($N = 2$), consisting of two wires in free space above a ground plane (see Fig. 3). Without loss of generality, all the metals are assumed to be perfect conductors and hence the interconnect structure is lossless. The following geometrical parameters are ascribed to the structure: wire radius $r_w = 0.5$ mm, wire separation $d = 5$ mm, height above the ground plane $h = 5$ cm. The conductors are 1-m long and terminated by 25-Ω and 100-Ω resistors at the near- and far-end sides, respectively.

The entries of the 2×2 p.u.l. inductance matrix are [27]

$$L_{11} = L_{22} = \frac{\mu_0}{2\pi} \cosh^{-1}\left(\frac{h}{r_w}\right), \tag{46a}$$

$$L_{12} = L_{21} = \frac{\mu_0}{4\pi} \ln\left(1 + 4\frac{h^2}{d^2}\right), \tag{46b}$$

where $\mu_0 = 4\pi \times 10^{-7}$ H/m is the vacuum permeability, while the p.u.l. capacitance matrix can be computed as

$$\mathbf{C} = \varepsilon_0 \mu_0 \mathbf{L}^{-1} = \varepsilon_0 \mu_0 \frac{1}{L_{11}^2 - L_{12}^2} \begin{bmatrix} L_{11} & -L_{12} \\ -L_{12} & L_{11} \end{bmatrix}, \tag{47}$$

where $\varepsilon_0 = 8.854 \times 10^{-12}$ F/m is the vacuum permittivity. Therefore,

$$\mathbf{L} = \begin{bmatrix} 1059.7 & 599.4 \\ 599.4 & 1059.7 \end{bmatrix} \text{ nH/m}, \tag{48}$$

$$\mathbf{C} = \begin{bmatrix} 15.44 & -8.73 \\ -8.73 & 15.44 \end{bmatrix} \text{ pF/m}. \tag{49}$$

Now suppose that the vertical position h is a uniformly distributed random variable expressed as

$$h(\xi) = \bar{h} + \Delta h\ \xi, \tag{50}$$

where $\bar{h} = 5$ cm is the nominal value, Δh is the semi-interval of variation and ξ is a normalized uniform random variable having a constant probability density function of $w(\xi) = 1/2$ in the interval $[-1, 1]$. The entries of the p.u.l. inductance (46) and capacitance (47) matrices are a function of h (and therefore of ξ) and can be expanded in terms of Legendre polynomials, which represent the optimal choice for uniform variability [7]. For instance, for $\Delta h = 4.5$ cm, a second-order expansion (i.e., $p = 2$), commonly selected in practical applications, produces

$$\hat{\mathbf{L}}(\xi) \approx \begin{bmatrix} 1020.7 & 561.5 \\ 561.5 & 1020.7 \end{bmatrix} \phi_0(\xi) + \begin{bmatrix} 132.7 & 131.0 \\ 131.0 & 132.7 \end{bmatrix} \phi_1(\xi) + \begin{bmatrix} -41.2 & -39.7 \\ -39.7 & -41.2 \end{bmatrix} \phi_2(\xi) \quad \text{nH/m} \tag{51a}$$

and

$$\hat{\mathbf{C}}(\xi) \approx \begin{bmatrix} 15.77 & -8.45 \\ -8.45 & 15.77 \end{bmatrix} \phi_0(\xi) + \begin{bmatrix} -0.76 & -0.67 \\ -0.67 & -0.76 \end{bmatrix} \phi_1(\xi) + \begin{bmatrix} 0.41 & 0.32 \\ 0.32 & 0.41 \end{bmatrix} \phi_2(\xi) \quad \text{pF/m}, \tag{51b}$$

where $\{\phi_{0,1,2}\}$ are the first three normalized Legendre polynomials, i.e.

$$\phi_0(\xi) = 1, \tag{52a}$$

$$\phi_1(\xi) = \sqrt{3}\,\xi, \tag{52b}$$

$$\phi_2(\xi) = \sqrt{5}/2\,(3\xi^2 - 1), \tag{52c}$$

and the expansion coefficients are computed according to (4) and (3) by numerically evaluating the integrals $\frac{1}{2}\int_{-1}^{1} L_{ij}(\xi)\phi_k(\xi)d\xi$ and $\frac{1}{2}\int_{-1}^{1} C_{ij}(\xi)\phi_k(\xi)d\xi$, for $i, j = 1, 2$ and $k = 0, 1, 2$.

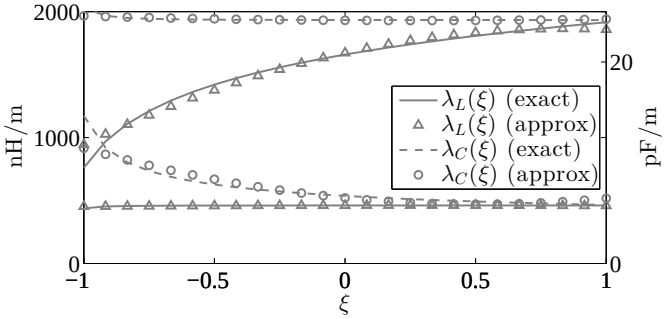

Fig. 4. Comparison between the eigenvalues of $\hat{\mathbf{L}}$ and $\hat{\mathbf{C}}$, expressed by (51) and plotted as a function of ξ, and those of the original parameters $\mathbf{L}$ and $\mathbf{C}$.

As discussed in Section IV-B, both $\hat{\mathbf{L}}$ and $\hat{\mathbf{C}}$ have to be PD $\forall \xi \in [-1, 1]$ for the augmented matrices to be guaranteed to describe a passive system. Fig. 4 displays the eigenvalues, denoted as λ_L and λ_C, of the original parameters $\mathbf{L}$ and $\mathbf{C}$ (lines) as a function of ξ, as well as those of the approximated parameters $\hat{\mathbf{L}}$ and $\hat{\mathbf{C}}$ (markers). The plot shows that the above condition is fulfilled, i.e. the approximated parameters are accurate enough to retain the positive-definiteness of the original ones. According to (8) and (9), the 6×6 augmented p.u.l. matrices are

$$\tilde{\mathbf{L}} = \begin{bmatrix} 1020.7 & 561.5 & 132.7 & 131.0 & -41.2 & -39.7 \\ 561.5 & 1020.7 & 131.0 & 132.7 & -39.7 & -41.2 \\ 132.7 & 131.0 & 983.9 & 526.0 & 118.7 & 117.1 \\ 131.0 & 132.7 & 526.0 & 983.9 & 117.1 & 118.7 \\ -41.2 & -39.7 & 118.7 & 117.1 & 994.4 & 536.2 \\ -39.7 & -41.2 & 117.1 & 118.7 & 536.2 & 994.4 \end{bmatrix} \frac{\text{nH}}{\text{m}}, \tag{53a}$$

whose eigenvalues are 1851.1, 1632.5, 1139.0, 455.2, 460.5, 459.6 [nH/m], and

$$\tilde{\mathbf{C}} = \begin{bmatrix} 15.77 & -8.45 & -0.76 & -0.67 & 0.41 & 0.32 \\ -8.45 & 15.77 & -0.67 & -0.76 & 0.32 & 0.41 \\ -0.76 & -0.67 & 16.14 & -8.17 & -0.68 & -0.60 \\ -0.67 & -0.76 & -8.17 & 16.14 & -0.60 & -0.68 \\ 0.41 & 0.32 & -0.68 & -0.60 & 16.03 & -8.25 \\ 0.32 & 0.41 & -0.60 & -0.68 & -8.25 & 16.03 \end{bmatrix} \frac{\text{pF}}{\text{m}}, \tag{53b}$$

whose eigenvalues are 6.12, 6.90, 10.06, 24.16, 24.21, 24.45 [pF/m]. Therefore, $\tilde{\mathbf{L}}$ and $\tilde{\mathbf{C}}$ are indeed both PD, their eigenvalues all being positive.

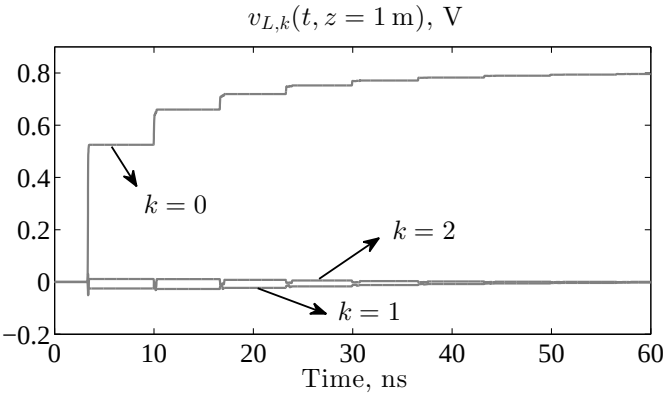

Fig. 5. Coefficients of the transient voltage at the load for the passive interconnect structure of Fig. 3.

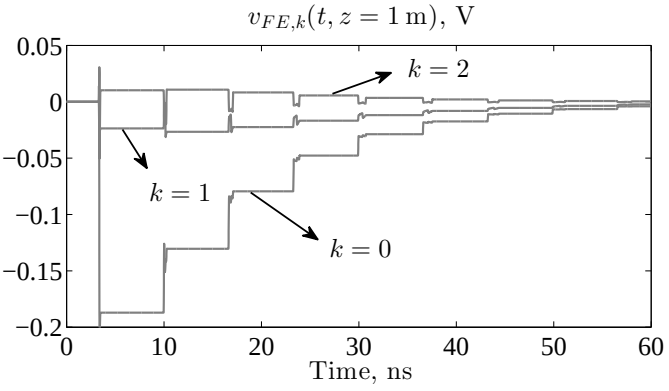

Fig. 6. Coefficients of the transient far-end crosstalk for the passive interconnect structure of Fig. 3.

A transient simulation is performed, where one line is considered to be active, and hence, a 1-V ramped step with a risetime of 50 ps is injected at its near end. After application of the augmentation as described before, leading to the matrices (53), each of the two stochastic voltages along the conductors in Fig. 3 is translated into three deterministic voltage coefficients, yielding a total of six new signals. For instance, the voltage transmitted to the load is described by its three corresponding gPC coefficients $v_{L,k}(t, z = 1\,\mathrm{m})$, $k = 0, 1, 2$, which are shown in Fig. 5 and correspond to three of the six terminal voltages of the augmented line. The remaining three terminal voltages, denoted as $v_{FE,k}$ and displayed in Fig. 6, represent the coefficients for the far-end crosstalk. It can be clearly observed that these responses converge to stable levels. According to the general properties of the gPC expansions [15], the coefficient $v_{L,0}(t)$ provides the gPC estimation of the average voltage at the load, while $v_{L,1}^2(t) + v_{L,2}^2(t)$ approximates its variance. The same properties apply of course to the coefficients of the far-end crosstalk.

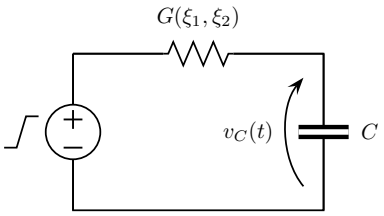

Fig. 7. Example of an RC circuit with a deterministic capacitance and a stochastic conductance.

B. RC Circuit

Next consider the lumped RC circuit of Fig. 7, consisting of a deterministic capacitor $C = 1$ nF and a wire resistor with conductance

$$G = \sigma \frac{\pi r^2}{L}. \tag{54}$$

The wire conductivity is $\sigma = 0.89$ MS/m (Nichrome), whereas its radius r and length L are two uniformly distributed random variables with mean value $\bar{r} = 0.1$ mm and $\bar{L} = 2.8$ cm, respectively, and 50% relative variation. As such, they can be expressed as

$$r = \bar{r} \cdot (1 + 0.5\xi_1), \tag{55a}$$
$$L = \bar{L} \cdot (1 + 0.5\xi_2), \tag{55b}$$

where ξ_1 and ξ_2 are two independent normalized uniform random variables with joint probability density function $w(\xi_1, \xi_2) = 1/4$ in the interval $[-1, 1] \times [-1, 1]$. A 1-V voltage step with risetime 50 ps is applied to the circuit.

The conductance (54) is now approximated by a second-order bivariate Legendre expansion (i.e., $p = n = 2$, leading to $P = 5$), as follows:

$$\begin{aligned}\hat{G}(\xi_1, \xi_2) = {} & 1.19\phi_0(\xi_1, \xi_2) + 0.63\phi_1(\xi_1, \xi_2) - 0.37\phi_2(\xi_1, \xi_2) \\ & + 0.08\phi_3(\xi_1, \xi_2) - 0.2\phi_4(\xi_1, \xi_2) + 0.10\phi_5(\xi_1, \xi_2),\end{aligned} \tag{56}$$

where $\{\phi_{0,1,2,3,4,5}\}$ are the first six normalized bivariate Legendre polynomials, i.e.

$$\phi_0(\xi_1, \xi_2) = 1, \tag{57a}$$
$$\phi_1(\xi_1, \xi_2) = \sqrt{3}\,\xi_1, \tag{57b}$$
$$\phi_2(\xi_1, \xi_2) = \sqrt{3}\,\xi_2, \tag{57c}$$
$$\phi_3(\xi_1, \xi_2) = \sqrt{5}/2\,(\xi_1^2 - 1), \tag{57d}$$
$$\phi_4(\xi_1, \xi_2) = 3\,\xi_1\xi_2, \tag{57e}$$
$$\phi_5(\xi_1, \xi_2) = \sqrt{5}/2\,(\xi_2^2 - 1), \tag{57f}$$

and the expansion coefficients are computed via the double integrals $\frac{1}{4}\int_{-1}^{1}\int_{-1}^{1} G(\xi_1, \xi_2)\phi_k(\xi_1, \xi_2)d\xi_1 d\xi_2$, for $k = 0, \ldots, 5$.

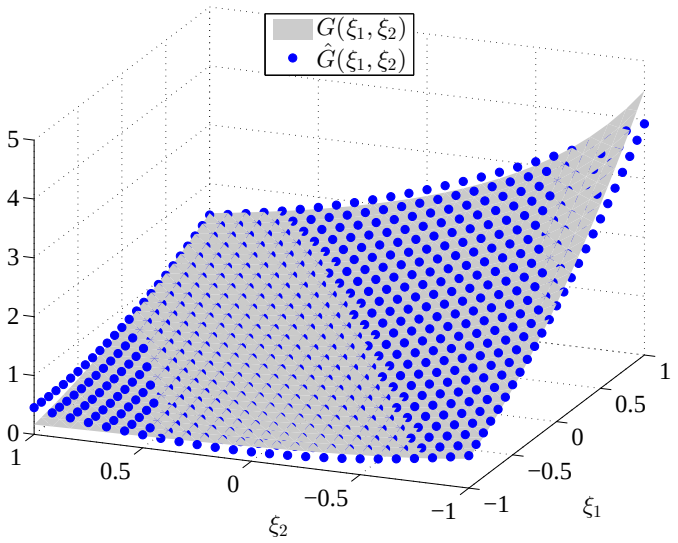

Fig. 8. Comparison between G and its approximation $\hat{G}$, expressed by (56).

According to the condition introduced in Section IV-A, (56) must be positive $\forall \xi_1, \xi_2 \in [-1, 1] \times [-1, 1]$ to ensure the passivity of the circuit model. Fig. 8 shows a comparison between the exact value of G, plotted as a function of ξ_1 and ξ_2 (gray surface), and the approximation provided by $\hat{G}$ (blue dots). Since the approximation $\hat{G}$ preserves the PD property, we expect the corresponding circuit model to be passive. The augmented conductance matrix is

$$\tilde{\mathbf{G}} = \begin{bmatrix} 1.19 & 0.63 & -0.37 & 0.08 & -0.20 & 0.10 \\ 0.63 & 1.26 & -0.20 & 0.57 & -0.37 & 0.00 \\ -0.37 & -0.20 & 1.28 & 0.00 & 0.63 & -0.33 \\ 0.08 & 0.57 & 0.00 & 1.24 & -0.18 & 0.00 \\ -0.20 & -0.37 & 0.63 & -0.18 & 1.35 & -0.18 \\ 0.10 & 0.00 & -0.33 & 0.00 & -0.18 & 1.25 \end{bmatrix} \text{S}, \tag{58}$$

whose eigenvalues are 2.66, 1.67, 0.39, 1.13, 1.10, 0.63 [S]. Therefore, $\tilde{\mathbf{G}}$ is PD and the overall augmented network passive. This is confirmed by the stability of the transient response in Fig. 9, which shows the six gPC coefficients for the voltage across the capacitor, denoted with $v_{C,k}(t)$, $k = 0, \ldots, 5$. As before, the coefficient $v_{C,0}(t)$ is the mean value of the voltage across the capacitor, while the variance is given by the sum of the squares of the remaining coefficients.

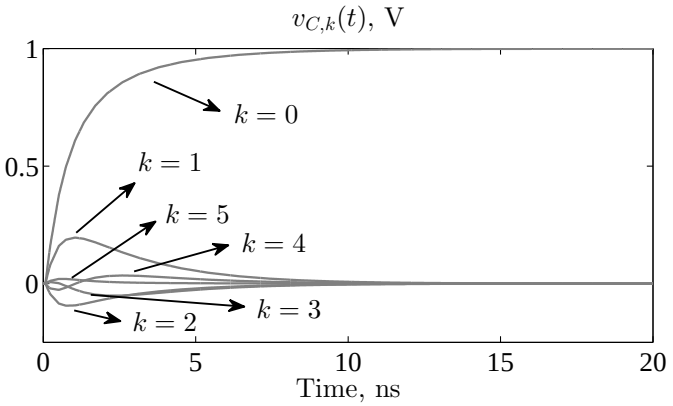

Fig. 9. Transient response for the passive RC circuit.

VI. Conclusions

This paper discusses the passivity of the deterministic circuit models generated by application of the gPC methodology, in combination with the SGM, to stochastic linear electrical networks consisting of both lumped and distributed elements. The gPC approach is based on the expansion of the stochastic parameters inside the governing equations in terms of suitable orthogonal polynomials. Subsequent application of the SGM produces deterministic problems described by larger sets of equations and whose solution provides the gPC coefficients of the unknown output variables, allowing an efficient extraction of statistical information.

For a SPICE-type implementation, such new augmented equations are interpreted as equivalent multi-terminal circuit elements or subcircuits. A deterministic, though larger instance of the original stochastic network is created, and a single simulation of such a new circuit allows to retrieve the sough-for gPC coefficients. However, although the application of this methodology to linear electrical circuits is well consolidated, a rigorous discussion about the passivity of the created models, which may affect the stability of time-domain simulations, had never been presented so far and therefore it is addressed for the first time in this paper.

The behavior of the new multi-terminal elements/subcircuits is defined by augmented matrices. On this basis, the paper provides a twofold contribution: i) it proves the general and necessary requirement that these matrices have to be PD to ensure the corresponding circuit models to be passive; ii) it proves the existence of a specific and sufficient condition for this requirement to be satisfied, i.e., the initial expansions of the electrical parameters have to preserve the passivity before the augmentation process is performed. Hence, it is established how the passivity in the end stems from the converge properties of the gPC expansions. The discussion is supported by numerical examples illustrating the theoretical results.

References

[1] T. Mikazuki and N. Matsui, "Statistical design techniques for high-speed circuit boards with correlated structure distributions," *IEEE Trans. Compon. Packag. Manuf. Technol. A*, vol. 17, no. 1, pp. 159–165, Mar. 1994.

[2] A. H. Zaabab, Qi-Jun Zhang, and M. Nakhla, "A neural network modeling approach to circuit optimization and statistical design," *IEEE Trans. Microw. Theory Tech.*, vol. 43, no. 6, pp. 1349–1358, Jun. 1995.

[3] Qiang Zhang, J. J. Liou, J. McMacken, J. Thomson, and P. Layman, "Development of robust interconnect model based on design of experiments and multiobjective optimization," *IEEE Trans. Electron Devices*, vol. 48, no. 9, pp. 1885–1891, Sep. 2001.

[4] G. S. Fishman, *Monte Carlo: Concepts, Algorithms, and Applications.* New York: Springer-Verlag, 1996.

[5] W. L. Loh, "On Latin hypercube sampling," *Ann. Stat.*, vol. 24, no. 5, pp. 2058–2080, 1996.

[6] H. Niederreiter, P. Hellekalek, G. Larcher, and P. Zinterhof, *Monte Carlo and Quasi-Monte Carlo Methods*. New-York: Springer-Verlag, 1998.

[7] D. Xiu and G. E. Karniadakis, "The Wiener-Askey polynomial chaos for stochastic differential equations," *SIAM Journal of Sci. Computation*, vol. 24, no. 2, pp. 619–622, 2002.

[8] Q. Su and K. Strunz, "Stochastic circuit modelling with Hermite polynomial chaos," *IET Electron. Lett.*, vol. 41, no. 21, pp. 1163–1165, Oct. 2005.

[9] S. Vrudhula, J. M. Wang, and P. Ghanta, "Hermite polynomial based interconnect analysis in the presence of process variations," *IEEE Trans. Comput.-Aided Des. Integr. Circuits Syst.*, vol. 25, no. 10, pp. 2001–2011, Oct. 2006.

[10] K. Strunz and Q. Su, "Stochastic formulation of SPICE-type electronic circuit simulation using polynomial chaos," *ACM Trans. Model. Comput. Simul.,* vol. 18, no. 4, pp. 15:1–15:23, Sep. 2008.

[11] N. Mi, S. X.-D. Tan, Y. Cai, and X. Hong, "Fast variational analysis of on-chip power grids by stochastic extended Krylov subspace method," *IEEE Trans. Comput.-Aided Des. Integr. Circuits Syst.*, vol. 27, no. 11, pp. 1996–2006, Nov. 2008.

[12] A. Rong and A. C. Cangellaris, "Interconnect transient simulation in the presence of layout and routing uncertainty," in *Proc. IEEE 20th Int. Conf. Elect. Perform. Electron. Packag. Syst.*, San Jose, CA, Oct. 2011, pp. 157–160.

[13] P. Sumant, Hong Wu, A. Cangellaris, and N. Aluru, "Reduced-order models of finite element approximations of electromagnetic devices exhibiting statistical variability," *IEEE Trans. Antennas Propag.*, vol. 60, no. 1, pp. 301–309, Jan. 2012.

[14] D. Spina, F. Ferranti, T. Dhaene, L. Knockaert, G. Antonini, and D. Vande Ginste, "Variability analysis of multiport systems via polynomial-chaos expansion," *IEEE Trans. Microw. Theory Tech.*, vol. 60, no. 8, pp. 2329–2338, Aug. 2012.

[15] D. Xiu, "Fast numerical methods for stochastic computations: a review," *Commun .Comput. Physics,* vol. 5, no. 2–4, pp. 242–272, Feb. 2009.

[16] I. S. Stievano, P. Manfredi, and F. G. Canavero, "Parameters variability effects on multiconductor interconnects via Hermite polynomial chaos," *IEEE Trans. Compon. Packag. Manuf. Techol.*, vol. 1, no. 8, pp. 1234–1239, Aug. 2011.

[17] I. S. Stievano, P. Manfredi, and F. G. Canavero, "Stochastic analysis of multiconductor cables and interconnects," *IEEE Trans. Electromagn. Compat.*, vol. 53, no. 2, pp. 501–507, May 2011.

[18] D. Vande Ginste, D. De Zutter, D. Deschrijver, T. Dhaene, P. Manfredi, and F. Canavero, "Stochastic modeling-based variability analysis of on-chip interconnects," *IEEE Trans. Compon. Packag. Manuf. Techol.*, vol. 2, no. 7, pp. 1182–1192, Jul. 2012.

[19] P. Manfredi, I. S. Stievano, and F. G. Canavero, "Alternative SPICE implementation of circuit uncertainties based on orthogonal polynomials," in *Proc. IEEE 20th Int. Conf. Elect. Perform. Electron. Packag. Syst.*, San Jose, CA, Oct. 2011, pp. 41–44.

[20] P. Manfredi, I. S. Stievano, and F. G. Canavero, "Expedite stochastic SPICE simulations by means of polynomial chaos," in *Proc. 16ème Colloque International sur la Compatibilité ElectroMagnétique*, Rouen, France, Apr. 2012.

[21] P. Manfredi, D. Vande Ginste, D. De Zutter, and F. G. Canavero, "Uncertainty assessment of lossy and dispersive lines in SPICE-type environments," submitted to *IEEE Trans. Compon. Packag. Manuf. Techol.*.

[22] P. Triverio, S. Grivet-Talocia, M. S. Nakhla, F. G. Canavero, and R. Achar, "Stability, causality, and passivity in electrical interconnect models," *IEEE Trans. Adv. Packag.*, vol. 30, no. 4, pp. 795–808, Nov. 2007.

[23] P. Manfredi, D. Vande Ginste, D. De Zutter, and F. G. Canavero, "Improved polynomial chaos discretization schemes to integrate interconnects into design environments," *accepted for publication in the IEEE Microw. and Wireless Compon. Lett.*.

[24] K. S. Suresh Kumar, *Electric Circuits and Networks.* Dorling Kindersley: New Delhi, 2009.

[25] G. Miano and A. Maffucci, *Transmission Lines and Lumped Circuits.* San Diego: Academic Press, 2001.
[26] F. Olyslager, *Electromagnetic Waveguides and Transmission Lines.* New York: Oxford University Press, 1999.
[27] C. R. Paul, *Analysis of Multiconductor Transmission Lines.* New York: Wiley, 1994.